Sains Malaysiana 51(12)(2022): 4087-4098
http://doi.org/10.17576/jsm-2022-5112-17

Enhanced Catalytic Palladium Embedded Inside Porous Silicon for Improved Hydrogen Gas Sensing

(Paladium Bermangkin Dipertingkat Terbenam di dalam Silikon Berliang untuk Pengesanan Gas Hidrogen yang Diperbaik)

ALHAN FARHANAH ABD RAHIM[1,*], NURUL SYUHADAH MOHD RAZALI[1], ROSFARIZA RADZALI[1], AINOKHILAH MAHMOOD[2], IRNI HAMIZA HAMZAH[1] & MOHAMED FAUZI PACKEER MOHAMED[3]

[1]*Centre for Electrical Engineering Studies, Universiti Teknologi MARA, Cawangan Pulau Pinang, Permatang Pauh Campus, 13500 Pulau Pinang, Malaysia*
[2]*Department of Applied Science, Universiti Teknologi MARA, Cawangan Pulau Pinang, 13500 Permatang Pauh, Pulau Pinang, Malaysia*
[3]*School of Electrical and Electronic Engineering, Engineering Campus, Universiti Sains Malaysia, 14300 Nibong Tebal, Pulau Pinang, Malaysia*

Received: 13 April 2022/Accepted: 20 August 2022

ABSTRACT

In this work, we reported on room temperature porous silicon (PS) and embedding PS using simple and economical techniques of electrochemical etching and thermal evaporation. The PS substrate was prepared using the technique of electrochemically etching the n-type Si (100) wafer at a constant current density of 10 mA/cm^2 for 10 min under the illumination of incandescent white light. After PS formation, Ge pieces were thermally evaporated onto the two PS substrates in a vacuum condition. This was then followed by the deposition of the ZnO layer onto the Ge/PS substrate by the same method using commercial 99.9% pure ZnO powders. The three samples were identified as PS, Ge/PS and ZnO/Ge/PS samples, respectively. Pd finger contacts were deposited on the PS and embedding PS (Ge/PS and ZnO/Ge/PS) to form Pd on PS hydrogen sensors using RF magnetron sputtering. SEM and EDX suggested the presence of substantial Ge and ZnO inside the uniform circular pores for Ge/PS and ZnO/Ge/PS samples, respectively. Raman spectra showed that good crystalline Ge and ZnO nanostructures embedded inside the pores were obtained. For hydrogen sensing, Pd on ZnO/Ge/PS Schottky diode exhibited a dramatic change of current after exposure to H_2 as compared to PS and Ge/PS devices. It is observed that the sensitivity increased exponentially with the hydrogen flow rate for all the sensors. The ZnO/Ge/PS showed more sensitivity towards H_2 than that of PS and Ge/PS especially at high flow rate of H_2 with higher current gain (69.11) and shorter response (180 s) and recovery times (30 s).

Keywords: Ge; H_2 sensor; porous silicon; thermal evaporation; ZnO

ABSTRAK

Dalam kajian ini, kami melaporkan silikon berliang (PS) dan PS terbenam menggunakan teknik mudah dan murah secara elektrokimia dan penyejatan terma pada suhu bilik. Substrat PS telah disediakan menggunakan teknik pengelasan elektrokimia wafer Si (100) jenis-n pada ketumpatan arus malar 10 mA/cm^2 selama 10 minit di bawah pencahayaan cahaya putih pijar. Selepas pembentukan PS, kepingan Ge disejat secara terma ke dua substrat PS dalam keadaan vakum. Ini diikuti dengan pemendapan lapisan ZnO ke substrat Ge/PS dengan kaedah yang sama menggunakan serbuk ZnO tulen komersial 99.9%. Ketiga-tiga sampel tersebut telah dikenal pasti sebagai sampel PS, Ge/PS dan ZnO/Ge/PS. Sentuhan berbentuk jari daripada Pd didepositkan pada PS dan PS terbenam (Ge/PS dan ZnO/Ge/PS) untuk membentuk Pd di atas penderia hidrogen PS dengan menggunakan teknik RF magnetron terpercik. SEM dan EDX mencadangkan kehadiran Ge dan ZnO yang besar di dalam liang bulat seragam masing-masing untuk sampel Ge/PS dan ZnO/Ge/PS. Spektrum Raman menunjukkan bahawa struktur nano Ge dan ZnO kristal yang baik yang tertanam di dalam liang telah diperoleh. Untuk penderiaan hidrogen, Pd pada diod Schottky ZnO/Ge/PS menunjukkan perubahan dramatik arus selepas pendedahan kepada H_2 berbanding dengan peranti PS dan Ge/PS. Diperhatikan bahawa kesensitifan meningkat secara eksponen dengan kadar aliran hidrogen untuk semua sensor. ZnO/Ge/PS menunjukkan lebih kesensitifan terhadap H_2 berbanding PS dan Ge/PS terutamanya pada kadar aliran tinggi H_2 dengan perolehan arus yang lebih tinggi (69.11) dan tindak balas yang lebih pendek (180 s) dan masa pemulihan (30 s).

Kata kunci: Ge; penderia H_2; penyejatan terma; silikon berliang; ZnO

Introduction

Porous silicon (PS) conventionally attained by the anodisation of crystalline silicon, is a potential candidate for highly efficient gas sensors due to their large specific area, which enhances the adsorption of the sensing gas and which is workable at room temperature (Kareem, Hussein & Abdul Hussein 2022; Mhamdi et al. 2022; Naderi, Hashim & Amran 2012). Embedding PS with Ge and metal oxide is an attractive candidate for a reduced extended defect density as it can enhance the stability of the PS sensor (Kanungo, Saha & Basu 2010). The simple and most commonly accepted theory of the semiconductor sensor operation mechanisms is described by the atoms and molecules of the gases interacting with semiconductor surfaces to influence the surface conductivity and surface potential (Cai & Park 2022; Polishchuk et al. 1998). Surface conductivity changes are mainly due to the changes in the free electron concentration due to the charge exchange between adsorbed species from the gas and the semiconductor surface. The charge exchange occurs in a thin layer below the gas-solid interface. As a consequence, for a high sensitivity gas detection, the semiconductor with a large specific area (surface area to volume ration) is desirable as it can produce a higher charge exchange rate. PS conventionally attained by the anodisation of crystalline silicon, is a potential candidate for highly efficient gas sensors mainly due to their large specific area, which can aid the enhancement of the adsorption of the sensing gas (Lewis et al. 2005; Mizsei 2007). In addition, the PS high chemical reactivity with the environment and the ease of porosity control by the variation of the anodisation parameters are suitable for various for sensing applications. Lower power consumption of PS-based devices in comparison with metal oxide or GaN gas sensors due to its capability in working at room temperature is another important advantage of this type of sensor. Additionally, it is easy to fabricate sensors using PS with the compatibility to cheap silicon IC technology.

One way to enhance gas sensitivity is by depositing a catalytic metal on the gate of the field effect structure. The selection of metal depends on the nature of the gas to be detected. A hydrogen sensitive gas sensor can be obtained by using palladium as gate metal in MOSFET structures (Hérino 2000; Jeske et al. 1995). Palladium is well known as it improves the surface activity towards hydrogen through its catalytic properties with regard to the dissociation of hydrogen molecules (Kanungo, Saha & Basu 2010). The coupling of the developed PS surface and high palladium catalytic activity for hydrogen seems to be a promising feature in creating a novel class of hydrogen gas sensors. Hydrogen (H_2) is one of the most dangerous and combustible gases. It has a great of flammability potential in air, which is about 4-75 % by volume and the lowest limit of H_2 concentration in air to cause explosion is 4.65 % (Boon-Brett et al. 2010; Han, Han & Khatkar 2006). This makes it more flammable than other fuels. Therefore there is a need for a device which is capable of detecting low levels of H_2 (Grimes et al. 2003). Recently, studies were carried out to obtain gas sensors with small size, low response and recovery time that can work at near room temperature (Al-Hardan, Abdullah & Aziz 2010; Alwan, Abed & Rashid 2021; Mhamdi et al. 2022). Particularly, in silicon-based gas sensors, it was known that the large active area of etched and textured Si has good interaction with gas whereby PS-based gas sensors should have high sensitivity and can work at room temperature. However, the properties of PS layers often degrade with time, and this defies the requirement of durability of the gas sensor. Thin film metal oxides are the materials of choice for gas sensors due to their sensitivity to gas and physical and chemical stability in gas media (Kanungo, Saha & Basu 2010). However, metal oxide needs to operate at high temperature to provide low response and recovery time and high sensitivity of the sensors. To improve the interaction between hydrogen and semiconductor materials, Pt or Pd catalytic layers are used (Meng et al. 2022; Rahimi & Iraji zad 2007; Wu et al. 2022). Therefore, based on the properties of PS and metal oxide layers with Pd as contact, we examine the PS and embedded PS for hydrogen sensors which will have the combination that has sensitivity and stability potential. By using the low cost-controlled size PS as the substrate and embedding other materials inside it by thermal evaporation, one can expect double cost cutting with enhanced performance. In this work, we attempted to use low-cost PS and embedding Ge and ZnO inside the PS using the conventional technique of thermal evaporation with catalytic palladium contact to investigate their potential for H_2 gas sensing.

Experimental procedures formation of porous silicon

The experiment began with the wet chemical etching of n-type <100>-oriented silicon wafers with a resistivity of 1-10 cm, by the standard Radio Corporation of America (RCA) technique. The wafers were electrochemically etched to create PS. The setup for the electrochemical anodization procedure to generate the PS is shown schematically in Figure 1. A handmade Teflon cell was utilised in the procedure, with a 1 cm × 1 cm Si wafer

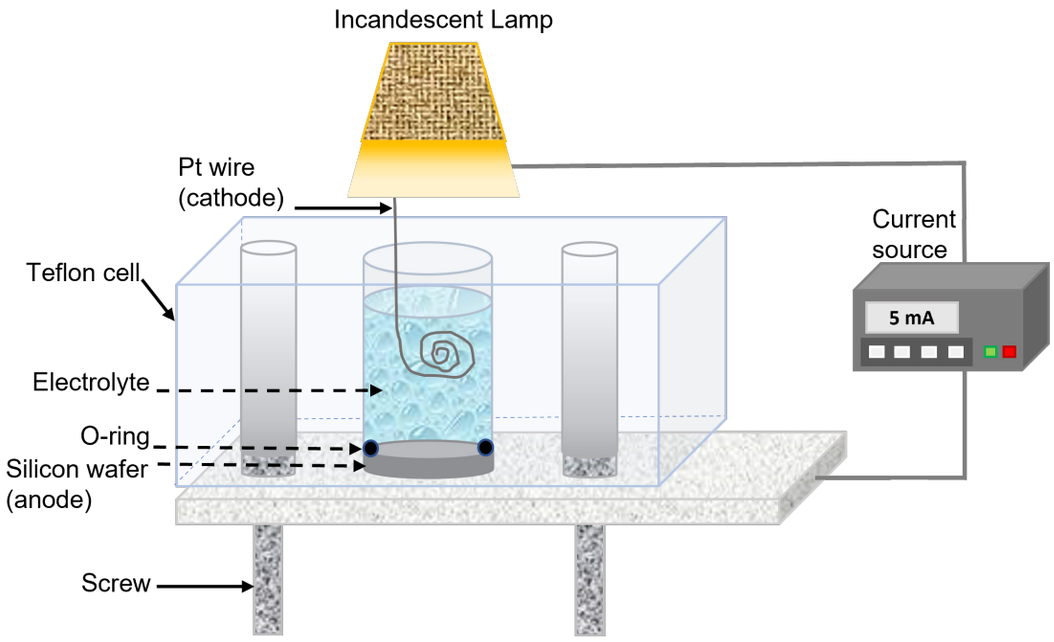

FIGURE 1. Schematic diagram of electrochemical etching setup to form PS

attached to the cell with an O-ring. The Si wafer acted as anode and Pt wire as cathode, respectively. The electrolyte used was made up of a ratio of 1:4 by the volume of 49% aqueous Hydrofluoric (HF) acid and 95% ethanol. A constant current density, J = 10 mA/cm^2 (provided by a Keithley 220 programmable current source) was employed for the electrochemical etching procedure for 10 minutes under the illumination of a 20 W incandescent lamp. The procedure was performed at room temperature. After the etching was completed, the samples were cleaned with deionized water and dried in the ambient air.

PREPARATION OF THE EMBEDDED PS STRUCTURES AND HYDROGEN GAS SENSOR

After the PS creation, commercial Ge pieces with a purity of 99.999% were thermally evaporated onto two PS substrates in a vacuum with a background pressure of 3.4 10^{-5} Torr using an Edwards Auto 306 thermal Evaporator unit. The ZnO layer was subsequently deposited onto the PS substrate using the same procedure as before, using commercial 99.9% pure ZnO powders. The three samples were labelled as PS, Ge/PS and ZnO/Ge/PS samples, respectively. The fabrication of the catalytic hydrogen gas sensor in this work begins with the deposition of Pd Schottky contact onto the PS by using RF magnetron sputtering systems. The Schottky contacts were patterned on the PS via a finger metal mask. Pd was chosen because of its catalytic characteristic which is suitable for hydrogen gas sensing, and also due to its better electrical properties and thermal stability when operating at high temperatures. The potential application of PS as hydrogen gas sensor was also investigated. The device was placed in a sealed chamber under a controlled flux of gases coming from a certified cylinder. The sensitivity measurement was conducted by measuring the I-V at different flow rates of H_2 passing into the chamber.

CHARACTERIZATION

The structural analyses of the samples were carried out using Scanning Electron Microscopy (SEM, JOEL JSM-6460LV), energy dispersive X-ray analysis (EDX). The experiments of gas sensing were carried out in a home-made gas chamber. 2% H_2 in N_2 was used throughout the experiments. The experimental setup of the gas sensor is depicted schematically in Figure 2. The characterization of the hydrogen sensor was done for PS and embedding PS samples (Ge/PS and ZnO/Ge/PS) deposited with palladium contact. Five different flow rates of 2% H_2 in N_2 gas were used in the experiments staring from

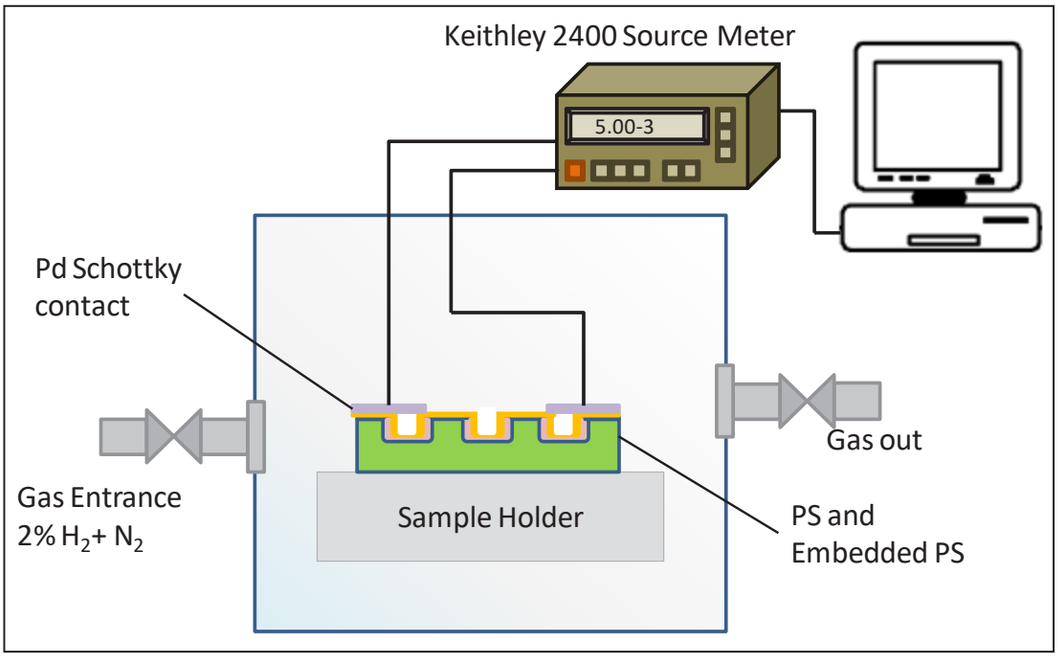

FIGURE 2. The schematic diagram of hydrogen gas sensing measurement setup

30 to 150 sccm. The test samples were placed into the chamber with wires connected from the probes to the Keithley model 2400 to measure the current-voltage (*I-V*) characteristics of the sample. All measurements were taken at room temperature.

RESULTS AND DISCUSSION

SURFACE MORPHOLOGY

Figure 3 shows the SEM micrographs of the three samples, with Figure 3(a) representing the initial Si wafer prior to anodization. Figure 3(b) shows that after anodizing in ethanoic HF solution for 10 min, the dissolution of silicon occurred in which a uniform network of circular pores of 500 nm to 700 nm was obtained on the Si surface. It may alternatively be thought of as a network of pores encasing a nanocrystalline skeleton (quantum sponge). PS has a very large internal surface area due to its unique structure, which induces a high level of adsorption. The holes in Figure 3(c) and 3(d) have been covered by Ge and ZnO deposition, respectively. For the Ge/PS and ZnO/Ge/PS samples, the EDX on the right side of the SEM indicated the presence of Ge and ZnO inside the pores. The Ge and ZnO peaks are quite prominent, suggesting that they cannot come from the scattered clusters on the porous structure, but could instead come from those located or embedded inside the PS. As previously demonstrated in our Ge/PS work, the presence of substance (Ge or GeO_2) in the pores of Figure 3(c) can be observed.

The large surface area is needed for highly effective gas sensor. The rougher surface of the porous structure is an advantage which translates to higher surface to volume ratio. The surface morphologies of the PS and embedding PS shown by Atomic Force Microscopy (AFM) result in the previous reported work (Abd Rahim et al. 2012) have shown that the trend of increasing island height was observed for the first layer deposition onto PS, while it decreased after the second layer deposition of the ZnO layer. This most likely suggests that the surface of the PS got rougher during the first layer deposition (Ge) as it attempted to penetrate further into the pore, and that after the second layer deposition (ZnO), the bumps were healed, or the pores were covered with the first layer. In addition, the good crystalline quality of the embedding samples can be observed by the significant Raman peaks observed at approximately 290 cm^{-1} and 520 cm^{-1}, corresponding to the Ge-Ge and Si-Si optical phonon modes, respectively

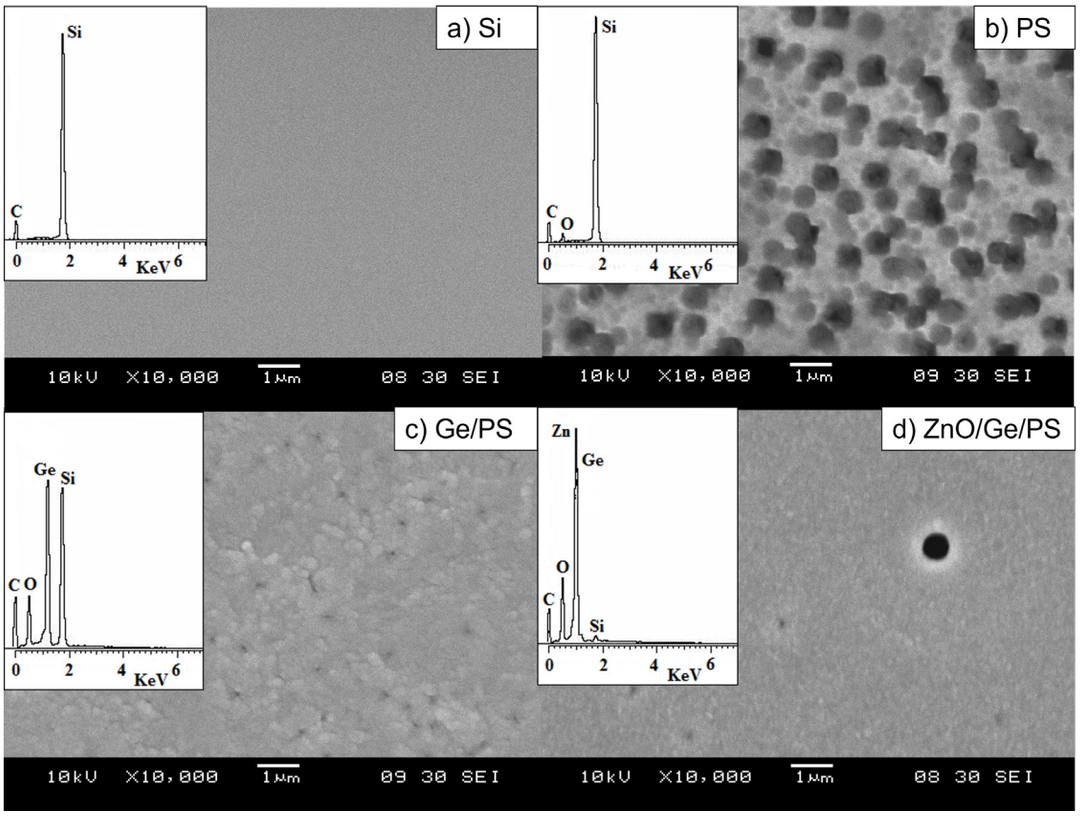

FIGURE 3. SEM images and EDX of the samples a) Si, b) PS, c) Ge/PS and d) ZnO/Ge/PS

(Abd Rahim et al. 2012) as shown in Figure 4. When the PS was embedded with Ge (Ge/PS), a very sharp Ge peak appeared, indicating that good nanocrystalline Ge had been deposited onto the PS. When compared to the host PS sample, the Ge/PS sample has a lower peak intensity of the Si-Si LO mode at 519.8 cm^{-1} with a peak shift of 0.5 cm^{-1}. This implies that the porous structure serves as a sink for threading dislocations and accommodates strain during the Ge layer deposition. Between 300 cm^{-1} and 520 cm^{-1}, there is no evidence of Si-Ge alloy mode, indicating that intermixing at the Ge/Si interfaces is minimal. When the second layer of ZnO was deposited, the Ge peak became asymmetrically broadened and shifted to a lower frequency with an estimated Ge crystallite size of about 1 nm. The presence of the tensile residual stress of the Ge on PS is indicated by the red shift of the Ge peak compared to that of the bulk Ge. This is consistent with the prediction of the phonon confinement theory for small nanocrystals (Kashtiban et al. 2010), which states that as the average size decreases, the Raman peak broadens and shifts slightly to lower frequencies. The ZnO/Ge/PS exhibits wurtzite hexagonal phase characteristics, with ZnO peaks at 376 cm^{-1}, 406 cm^{-1}, 438 cm^{-1}, 572 cm^{-1}, and 589 cm^{-1}, which correspond to A1(TO), E1(TO), E2(high), A1(LO), and E1(LO), respectively (Abd Rahim et al. 2012).

CHARACTERISTICS OF PS AND EMBEDDED PS AS HYDROGEN SENSORS

Figure 5(a) shows the *I-V* characteristics of the Pd/PS, Pd/Ge/PS and Pd/ZnO/Ge/PS hydrogen gas sensors operating in 150 sccm flow rate of 2% H_2 in N_2 gas at room temperature. The three sensors were found to show good Schottky behaviour. A remarkable increase of the current was observed when the devices were exposed to hydrogen.

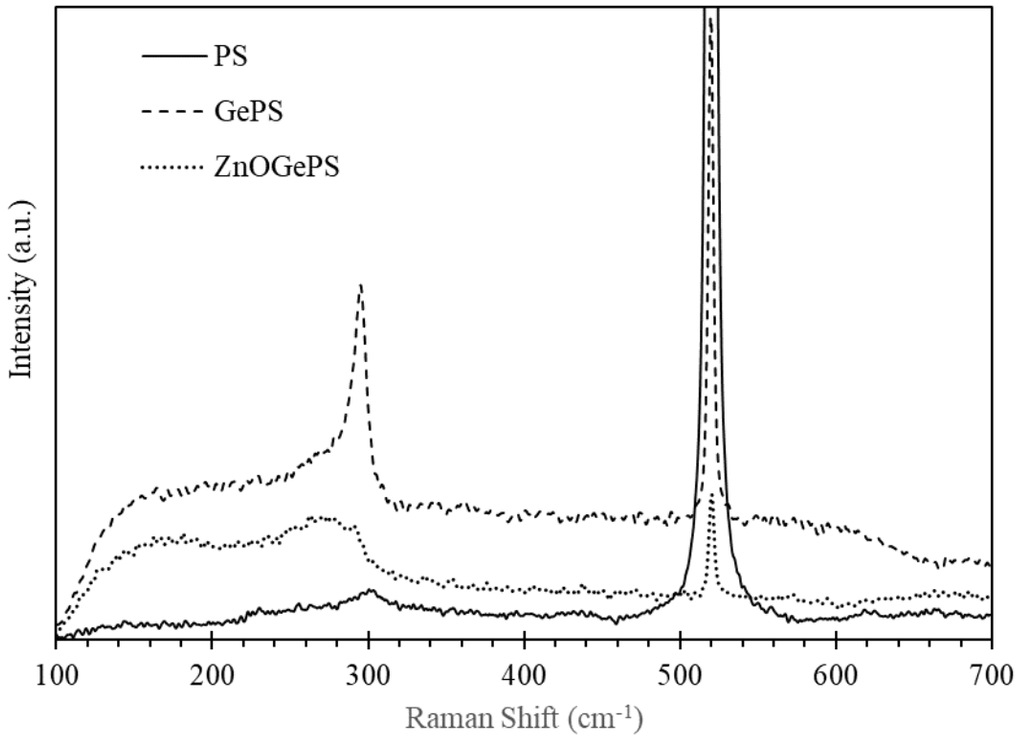

FIGURE 4. Raman spectra of the PS, Ge/PS and ZnO/Ge/PS taken at room temperature

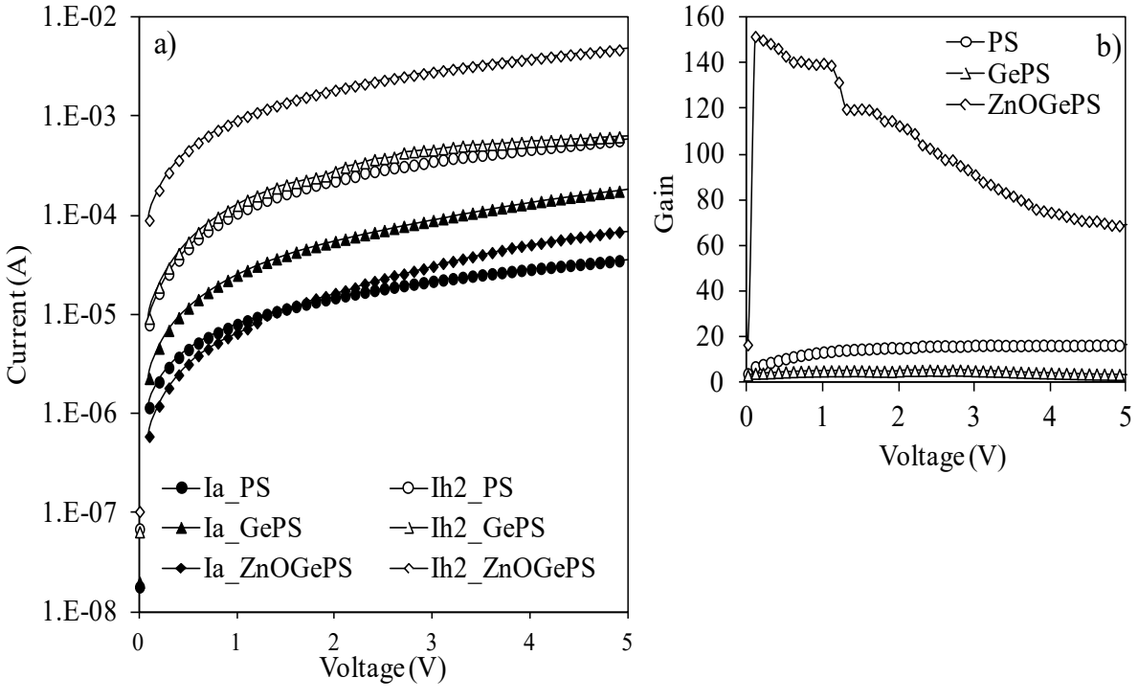

FIGURE 5. a) Room temperature *I-V* characteristics of the PS, Ge/PS and ZnO/Ge/PS hydrogen sensors under ambient air (I_a) and under 2% hydrogen adsorption (I_{h2}) at flow rate of 150 sccm. Also shown is b) the gain of the three sensors

In general, the ZnO/Ge/PS sample showed better response towards the gas flow rate (~ two orders of magnitude current changes) than that of the PS (just over one order of magnitude) and Ge/PS (only about two times increase). Figure 5(b) shows the response of the three sensors towards 2% hydrogen extracted from the ratio of the current under hydrogen adsorption to the current under ambient air. Particularly, at 5 V bias, the ZnO/Ge/PS sample obtained the highest gain of 69.11, followed by PS (16.32) and Ge/PS (3.45), respectively. This shows that PS is a good substrate for hydrogen adsorption. However, putting Ge is not suitable for hydrogen adsorption which decreased the response. On the other hand, embedding ZnO into Ge/PS substrate enhanced the response tremendously. This probably occurred through the use of the catalytic Pd on top of the ZnO/Ge/PS sample whereby reactivity increased, and more hydrogen was absorbed. Specifically, when hydrogen molecules pass through the Pd, they dissociate into atoms or ions, which leads to better and stronger interaction between hydrogen atoms or ions with oxygen species adsorbed on the ZnO surface and this leads to the enhanced response and sensitivity. Besides, the Pd catalytic layer always plays unambiguously positive role in increasing the selectivity of fabricated devices to hydrogen even if hydrogen is present in a mixture with other gases. In addition, the embedding ZnO on the high surface area of PS allows a wider area for hydrogen absorption and subsequently increased the sensitivity and stability (Aroutiounian et al. 2009).

Table 1 summarizes the SBH, ideality factor, gain and series resistance extracted from the *I-V* measurement of the three sensors. Assuming that the thermionic emission is the most predominant mechanism, from *I-V* characteristics, the Schottky barrier heights for the three samples for 150 sccm flow rate of hydrogen can be calculated based on the thermionic emission theory. The thermionic emission theory is the well-known model used to study the forward *I-V* characteristics of a Schottky diode. According to this theory, the diode current, I_d is described by the following equation (Jandow et al. 2010; Rhoderick et al. 1988):

$$I_d = I_0 \exp\left(\frac{qV_d}{nkT}\right)\left[1-\exp\left(\frac{-qV_d}{kT}\right)\right] \quad (1)$$

where V_d is the voltage across the diode; n is the ideality factor (which may depend on the temperature and independent on the voltage); k is the Boltzman constant; and I_o is the saturation current given by:

$$I_0 = AA^{**}T^2 \exp\left[\frac{-q\varphi_B}{kT}\right] \quad (2)$$

where q is the electron charge; T is the temperature; A is the contact area; A^{**} is the effective Richardson constant; and ϕ_B is the Schottky barrier height. The saturation current, I_0 is mainly determined by the barrier height ϕ_B and the effective Richardson constant A^{**}. Equation (1) at $V_d >> 3kT/q$, can be simplified to:

$$I_d = I_0 \exp\left(\frac{qV_d}{nkT}\right) \quad (3)$$

The theoretical value of A^{**} can be calculated using $A^{**} = 4pm^*qk^2/h^3$ where m^* is the effective mass; k is Boltzmann constant; and h is Planck's constant. The plot of $ln\ I_d\ vs\ V_d$ will give a straight line with a slope of $q/(nkT)$, and the intercept with y-axis will yield I_o, in which Schottky barrier height, ϕ_B can be obtained using Equation (2) and the ideality factor can be extracted from the slope. The effect of series resistance R_s can be modeled as a series combination of a resistor and a diode. The voltage V_d across the diode is given by $V_d = V\text{-}IRs$ where I is the current flowing through the resistor. Equation (3) with the effect of series resistance will be written as:

$$I_d = I_0 \exp\left(\frac{q(V-IR_s)}{nkT}\right) \quad (4)$$

From this, R_s can be estimated from the *I-V* characteristics of the diode at high forward bias as:

$$R_s = \left(\frac{\partial I}{\partial V}\right)^{-1} \quad (5)$$

The values of the barrier heights of the three samples under ambient and hydrogen adsorption are shown in Table 1. The barrier height could be seen to decrease with hydrogen exposure in the sensors. The difference of the SBH is large (0.08 eV) in the ZnO/Ge/PS sample than that of PS (0.04 eV) and Ge/PS (0.03 eV) which indicates that the ZnO/Ge/PS sample was more sensitive to hydrogen. Decreases in barrier height are justified by the increase in the current and the decrease of the series resistance upon the H_2 exposure.

TABLE 1. The Schottky barrier height, ideality factor, gain and series resistance for PS and Embedded PS as hydrogen sensors

Sample	SBH (eV)	Ideality factor (n)	Gain at 5V	R_s at 5V(KΩ)
PS_air	0.821	1.62	16.32	140.00
PS_h2	0.784	1.41		8.57
Ge/PS_air	0.816	1.42	3.45	27.40
Ge/PS_h2	0.785	1.36		7.94
ZnO/Ge/PS_air	0.847	1.47	69.11	72.00
ZnO/Ge/PS_h2	0.763	1.04		1.04

For an ideal Schottky diode behaviour, the ideality factor (*n*) should be nearly equal to unity. Nonetheless, in a real situation, it may increase when the effects of series resistance and leakage current become significant. It may be observed that the ideality factor for the three Schottky diodes decreased with hydrogen exposure. The values of (*n*) were almost in unity for the Pd/ZnO/Ge/PS showing that the good electrical contact of Pd on the ZnO surface constituted to higher current and lower resistance. The slightly higher ideality factors for PS and Ge/PS may be due to the existence of a large number of surface states characterizing the nano-porous layers constituting the diodes and the high resistive nature of the PS surfaces.

The series resistances evaluated from *I-V* curves for the three devices measured at 300K before and after the gas exposure with different flow rates, are shown in Figure 6(a) to 6(c). The series resistance decreased exponentially upon the introduction of different flow rates of 2% H_2 in N_2 gas for the three devices. However, the resistances for PS are very high compared with the embedded structures. Probably, the higher resistance was due to the oxidation of the PS surface.

Sensitivity is one of the important parameters that is normally used as an indicator to gauge the performance of a gas sensor. The sensitivity (*S*) was defined as in Equation (6) as the ratio of change in the current in the presence of hydrogen (I_{H2}-I_A) to that in air (I_A), at a fixed applied voltage. Sensitivity is one of the important parameters normally used to measure the performance of the gas sensor. The hydrogen detection sensitivity, *S*, is defined as:

$$S = \frac{I_{H_2} - I_{Air}}{I_{Air}} \tag{6}$$

where I_{H2} and I_{Air} are the current under H_2 exposure and under ambient air, respectively, at a fixed applied voltage. The expression of this H_2 sensitivity can be used for both forward and reverse current modes at a fixed applied voltage.

Figure 6(a) to 6(c) shows the variation of sensitivity with H_2 flow rate at room temperature for the three samples recorded at 5 V in forward current mode. One may observe that the sensitivity increased almost linearly with hydrogen flow rate for both sensors PS and Ge/PS for the range up to 90 sccm and then increased exponentially with the sensitivity of 5 and 2.5 at 150 sccm, respectively. For ZnO/Ge/PS, the sensitivity increases rapidly upon the introduction of gas and slowly reaches saturation (about 66) above 120 sccm. The ZnO/Ge/PS is more sensitive to hydrogen than that of PS and Ge/PS by a factor of 13 and 27, respectively, at flow rate of 150 sccm. This might be due to the increase of the coupling effect of the catalytic Pd with embedded ZnO and the increase of the PS surface area, which enable the enhancement of the adsorbate effects; this causes high activity in surface chemical reactions to take place (Korotcenkov & Cho 2010; Mareš, Krištofik & Hulicius 1995).

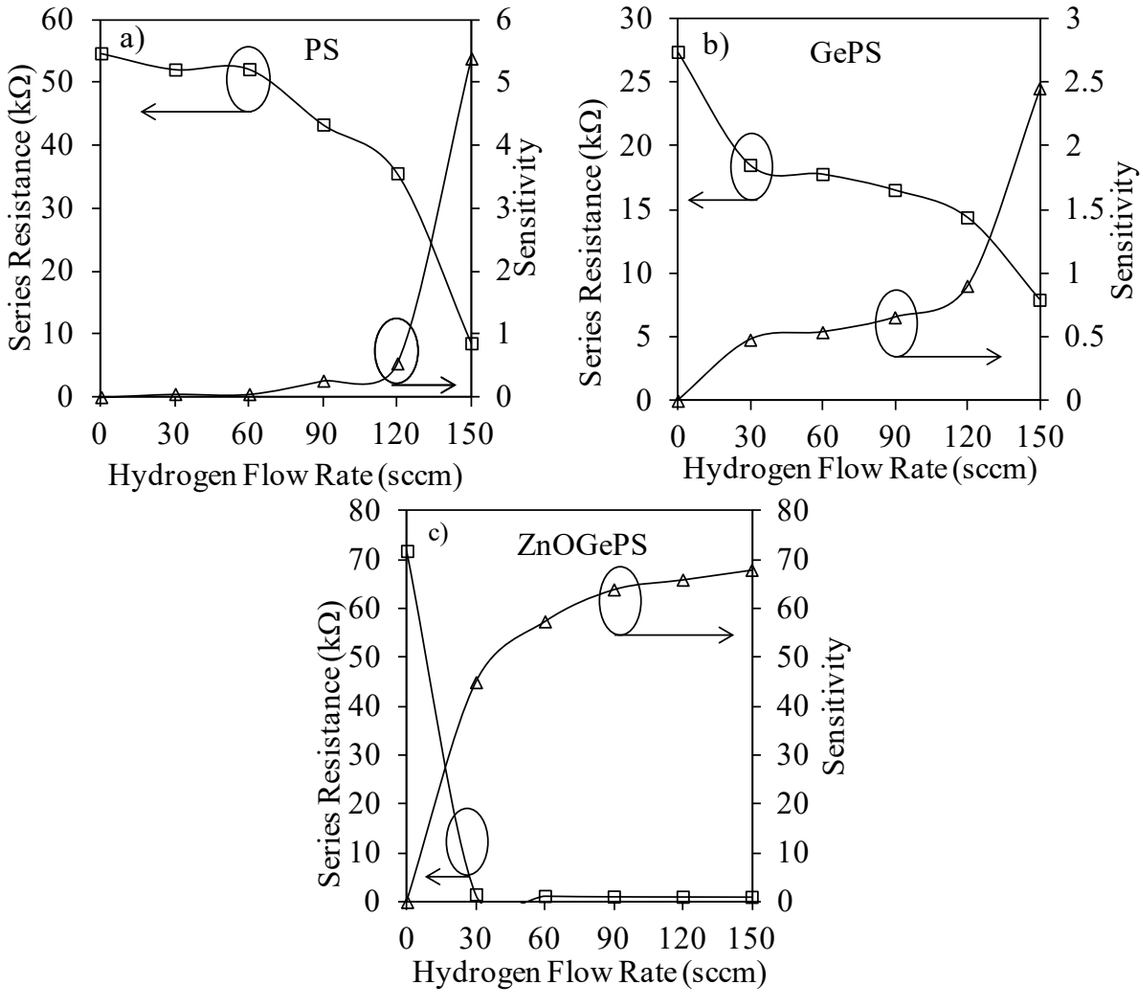

FIGURE 6. Series resistance and sensitivity as a function of hydrogen flow rate for the three devices: a) PS, b) Ge/PS and c) ZnO/Ge/PS

The results showed that the response of a PS sensor improves significantly when its surface is modified with metal oxide and Pd metal. During hydrogen sensing, hydrogen molecule decomposes to hydrogen atoms on the catalytic Pd surface and diffuse through the catalyst and reaches the Pd-ZnO PS interface. At this interface, these atoms polarize and give rise to a dipole layer, which in turn alters the work function of the Pd metal and subsequently decreases the SBH (Kanungo, Saha & Basu 2010; Rahimi & Iraji zad 2007). This observation coincides with the fact that porous substrate has a large specific area coupled with catalytic Pd and ZnO which stabilize the material (oxygen atoms will react with the remaining dangling electrons of the PS surface and passivate the defects states) (Kanungo, Saha & Basu 2010). This provides a sensitive large contact area, hence giving it a higher chance to react with gases and increase the sensitivity.

Figure 7 shows the consecutive current responses of the three devices with time at H_2 flow rate 150 sccm. The adsorption and desorption times were set at 300 s, respectively. Fresh air was flown in the chamber by using air pump to push out the hydrogen in between the different flows of H_2. The response time is defined as the time taken for the sensor to reach 90% of the saturation current from the initial value while the recovery time is defined as the time taken from the saturation current to reach 10% of its saturation current value after the contact of the test gas with the sensor surface.

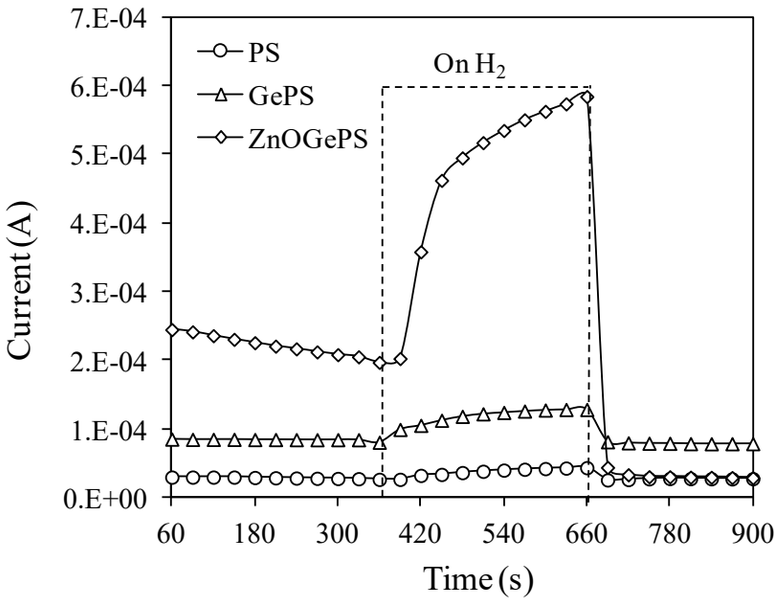

FIGURE 7. Current response towards H_2 flow rate of 150 sccm for the three devices

From the figure, both response and recovery times were less than 300 s on all the sensors. For example, the response times taken were 240 s, 270 s and 180 s for PS, Ge/PS and ZnO/Ge/PS. The recovery times were much faster with 60 s for PS and Ge/PS while only 30 s for the ZnO/Ge/PS, respectively, measured at 150 sccm of H_2 gas. Again, ZnO/Ge/PS showed an enhanced response towards H_2 compared to PS and Ge/PS by the higher current response at much shorter response and recovery times during the gas exposure.

The accurate fundamental mechanisms that cause a gas response are still debatable (Korotcenkov & Cho 2010), but the simplest and most commonly accepted theory of the semiconductor sensor operation mechanisms is that atoms and molecules of the gases interact with semiconductor surfaces to influence the surface conductivity and surface potential (Parkhutik 1999). The changes of the surface conductivity are primarily due to the changes in the free electron concentration as a result of the charge exchange between adsorbed species from the gas and the semiconductor surface. This charge exchange takes places in a thin layer below the gas to solid interface. Consequently, for a high sensitivity gas detection, a large specific area (surface area to volume ratio) semiconductor is necessary to produce a higher charge exchange rate. Thus, using porous substrates these interactions increased and dipoles layers become larger due to the large specific area. A decrease in SBH is observed upon the H_2 exposure due to the shift of the electrostatic potential of PS. This decrease in SBH would be in proportion to the hydrogen flow rate as has been observed above. The changes of the surface conductivity also change the Schottky barrier height, and then change in the electrical characteristic of the device. The change in the electric polarization ΔV is given by equation (7) (Johansson, Lundström & Ekedahl 1998).

$$\Delta V = \frac{\mu N_i \theta_i}{\varepsilon} \tag{7}$$

where μ is the effective dipole moment; N_i is the number of sites per area at the interface; θ_i is the coverage of hydrogen atoms at the interface; and ε is the dielectric constant. It is found that the higher the hydrogen flow rate, the greater the changes in ΔV, resulting in the greater change of the energy barrier height at the metal/semiconductor interface. As a result, the current through the Schottky barrier will change as well.

Conclusions

In conclusion, we successfully prepared PS and embedded PS nanostructures (Ge/PS and ZnO/Ge/PS) by using a simple and conventional technique of photo electrochemical etching and thermal evaporation. SEM

showed that the structures contained uniform circular-pores and EDX suggested the presence of substantial Ge and ZnO inside the pores for Ge/PS and ZnO/Ge/PS, respectively. Raman spectra showed that good crystalline Ge and ZnO nanostructures embedded inside the pores were obtained. Interestingly, Pd on ZnO/Ge/PS Schottky diode exhibited a dramatic change of current after the exposure to H_2 as compared to PS and Ge/PS devices. It is observed that the sensitivity increased exponentially with the hydrogen flow rate for all the sensors, and yet ZnO/Ge/PS showed more sensitivity towards H_2 than that of PS and Ge/PS especially at the high flow rate of H_2 with higher current and shorter response and recovery times. The results also suggest that PS is a good substrate for producing good crystalline Ge and ZnO/Ge nanostructures, and it acts as sink for threading dislocations and accommodates the strain for the Ge layer deposition on it. This shows that it is possible to grow high quality Si, Ge and ZnO nanostructures using the simple techniques of photo electrochemical etching and thermal evaporation for potential applications in gas sensing devices.

ACKNOWLEDGEMENTS

The author wishes to thank members of Universiti Teknologi MARA, Cawangan Pulau Pinang, the Nano-optoelectronics Lab, USM, and Department of Applied Science, Universiti Teknologi MARA, Cawangan Pulau Pinang, for their endless technical assistance. The financial support from the Universiti Teknologi MARA through MyRA Research Grant Scheme (600-RMC/GPM ST 5/3 (042/2021) and Universiti Teknologi MARA, Cawangan Pulau Pinang is gratefully acknowledged.

REFERENCES

Abd Rahim, A.F., Hashim, M.R., Rusop, M., Ali, N.K. & Yusuf, R. 2012. Room temperature Ge and ZnO embedded inside porous silicon using conventional methods for photonic application. *Superlattices and Microstructures* 52(5): 941-948.

Al-Hardan, N.H., Abdullah, M.J. & Abdul Aziz, A. 2010. Sensing mechanism of hydrogen gas sensor based on RF-sputtered ZnO thin films. *International Journal of Hydrogen Energy* 35(9): 4428-4434.

Alwan, A.M., Abed, H.R. & Rashid, R.B. 2021. Enhancing the temporal response of modified porous silicon-based CO gas sensor. *Solid-State Electronics* 181-182: 108019.

Aroutiounian, V., Arakelyan, V., Galstyan, V., Martirosyan, K. & Soukiassian, P. 2009. Hydrogen sensor made of porous silicon and covered by TiO_{2-x} or ZnO<Al> thin film. *IEEE Sensors Journal* 9(1): 9-12.

Boon-Brett, L., Bousek, J., Black, G., Moretto, P., Castello, P., Hübert, T. & Banach, U. 2010. Identifying performance gaps in hydrogen safety sensor technology for automotive and stationary applications. *International Journal of Hydrogen Energy* 35(1): 373-384.

Cai, Z. & Park, S. 2022. A superior sensor consisting of porous, Pd nanoparticle–decorated SnO_2 nanotubes for the detection of ppb-level hydrogen gas. *Journal of Alloys and Compounds* 907: 164459.

Grimes, C.A., Ong, K.G., Varghese, O.K., Yang, X., Mor, G., Paulose, M., Dickey, E.C., Ruan, C., Pishko, M.V., Kendig, J.W. & Mason, A.J. 2003. A sentinel sensor network for hydrogen sensing. *Sensors* 3(3): 69-82.

Han, C-H., Han, S-D. & Khatkar, S.P. 2006. Enhancement of H_2-sensing properties of F-doped SnO_2 sensorby surface modification with SiO_2. *Sensors* 6(5): 492-502.

Hérino, R. 2000. Nanocomposite materials from porous silicon. *Materials Science and Engineering: B* 69-70: 70-76.

Jandow, N.N., Yam, F.K., Thahab, S.M., Abu Hassan, H. & Ibrahim, K. 2010. Characteristics of ZnO MSM UV photodetector with Ni contact electrodes on poly propylene carbonate (PPC) plastic substrate. *Current Applied Physics* 10(6): 1452-1455.

Jeske, M., Schultze, J.W., Thönissen, M. & Münder, H. 1995. Electrodeposition of metals into porous silicon. *Thin Solid Films* 255(1): 63-66.

Johansson, M., Lundström, I. & Ekedahl, L.G. 1998. Bridging the pressure gap for palladium metal-insulator-semiconductor hydrogen sensors in oxygen containing environments. *Journal of Applied Physics* 84(1): 44-51.

Kanungo, J., Saha, H. & Basu, S. 2010. Pd sensitized porous silicon hydrogen sensor - Influence of ZnO thin film. *Sensors and Actuators B: Chemical* 147(1): 128-136.

Kareem, M.H., Hussein, H.T. & Abdul Hussein, A.M. 2022. Study of the effect of CNTs, and (CNTs-ZnO) on the porous silicon as sensor for acetone gas detection. *Optik* 259: 168825.

Kashtiban, R.J., Pinto, S.R.C., Bangert, U., Rolo, A.G., Chahboun, A., Gomes, M.J.M. & Harvey, A.J. 2010. Ge nanocrystals in alumina matrix: A structural study. *Journal of Physics: Conference Series* 209: 012060.

Korotcenkov, G. & Cho, B.K. 2010. Porous semiconductors: Advanced material for gas sensor applications. *Critical Reviews in Solid State and Materials Sciences* 35(1): 1-37.

Lewis, S.E., DeBoer, J.R., Gole, J.L. & Hesketh, P.J. 2005. Sensitive, selective, and analytical improvements to a porous silicon gas sensor. *Sensors and Actuators B: Chemical* 110(1): 54-65.

Mareš, J., Krištofik, J. & Hulicius, E. 1995. Influence of humidity on transport in porous silicon. *Thin Solid Films* 255 (1): 272-275.

Meng, X., Bi, M., Xiao, Q. & Gao, W. 2022. Ultra-fast response and highly selectivity hydrogen gas sensor based on Pd/SnO_2 nanoparticles. *International Journal of Hydrogen Energy* 47(5): 3157-3169.

Mhamdi, H., Azaiez, K., Fiorido, T., Benabderrahmane Zaghouani, R., Lazzari, J.L., Bendahan, M. & Dimassi, W. 2022. Room temperature NO2 gas sensor based on stain-etched porous silicon: Towards a low-cost gas sensor integrated on silicon. *Inorganic Chemistry Communications* 139: 109325.

Mizsei, J. 2007. Gas sensor applications of porous Si layers. *Thin Solid Films* 515(23): 8310-8315.

Naderi, N., Hashim, M.R. & Amran. T.S.T. 2012. Enhanced physical properties of porous silicon for improved hydrogen gas sensing. *Superlattices and Microstructures* 51(5): 626-634.

Parkhutik, V. 1999. Porous silicon - Mechanisms of growth and applications. *Solid-State Electronics* 43(6): 1121-1141.

Polishchuk, V., Souteyrand, E., Martin, J.R., Strikha, V.I. & Skryshevsky, V.A. 1998. A study of hydrogen detection with palladium modified porous silicon. *Analytica Chimica Acta* 375(3): 205-210.

Rahimi, F. & Iraji zad, A. 2007. Characterization of Pd nanoparticle dispersed over porous silicon as a hydrogen sensor. *Journal of Physics D: Applied Physics* 40(23): 7201-7209.

Rhoderick, E.H., Rhoderick, E.H., Williams, R.H. & Williams, R.H. 1988. *Metal-Semiconductor Contacts*. New York: Clarendon Press.

Wu, J., Xi, X., Zhu, W., Yang, Z., An, P., Wang, Y., Li, Y., Zhu, Y., Yao, W. & Jiang, G. 2022. Boosting photocatalytic hydrogen evolution via regulating Pt chemical states. *Chemical Engineering Journal* 442(Part 2): 136334.

*Corresponding author; email: alhan570@uitm.edu.my